

Supplementary Information

Investigating the Role of Halogen-Bonded Complex in Microsolvated $\text{Y}^-(\text{H}_2\text{O})_n + \text{CH}_3\text{I}$ S_N2

Reactions

Xiaoyan Ji, Chongyang Zhao Jing Xie*

^aKey Laboratory of Cluster Science of Ministry of Education, School of Chemistry and Chemical Engineering, Beijing Institute of Technology, Beijing 100081, China

Table S1-S10

Figure S1-S12

Table S1. Experimental studies of halophilic reaction that forms dihalogen anions.

nucleophile	reactant	dihalide product	halogen-bonded complex	reference
F ⁻	CF ₃ Br	BrF ⁻	[CF ₃ --Br--F] ⁻	¹ Viggiano, <i>J. Phys. Chem.</i> 1994
F ⁻	CF ₃ I	IF ⁻	[CF ₃ --I--F] ⁻	¹ Viggiano, <i>J. Phys. Chem.</i> 1994
F ⁻	CH ₃ Cl	ClF ⁻	[CH ₃ --Cl--F] ⁻	² Ervin, <i>J. Am. Chem. Soc.</i> 2001
F ⁻	CH ₃ I	IF ⁻	[CH ₃ --I--F] ⁻	³ Wester, <i>J. Phys. Chem. A</i> 2016
Cl ⁻	CH ₃ Br	BrCl ⁻	[CH ₃ --Br--Cl] ⁻	⁴ Viggiano, <i>J. Am. Chem. Soc.</i> 1995
Cl ⁻	CH ₃ I	ICl ⁻	[CH ₃ --I--Cl] ⁻	⁴ Viggiano, <i>J. Am. Chem. Soc.</i> 1995
Cl ⁻	CH ₃ F	ClF ⁻	[CH ₃ --F--Cl] ⁻	⁵ Ervin, <i>J. Am. Chem. Soc.</i> 2002
I ⁻	CH ₃ I	I ₂ ⁻	[CH ₃ --I--I] ⁻	⁴ Viggiano, <i>J. Am. Chem. Soc.</i> 1995
I ⁻	CH ₃ Cl	ICl ⁻	[CH ₃ --Cl--I] ⁻	⁶ Ervin, <i>J. Phys. Chem. A</i> 2004
I ⁻	CH ₃ Br	IBr ⁻	[CH ₃ --Br--I] ⁻	⁶ Ervin, <i>J. Phys. Chem. A</i> 2004
HO ⁻	CH ₃ I	IOH ⁻	[CH ₃ --I--OH] ⁻	⁷ Wester, <i>Faraday Discussion</i> , 2012

Table S2. Comparison of reaction energies^a for $\text{Nu}^- + \text{CH}_3\text{I} \rightarrow \text{NuCH}_3 + \text{I}^-$ S_N2 reaction (X = OH, F, Cl, Br) with different level of theory.

method	basis set	OH ⁻	F ⁻	Cl ⁻	Br ⁻	reference
B97-1	ECP/d	-68.8 (-64.9) [-66.8]	-46.8 (-45.1) [-45.2]	-13.1 (-12.4) [-12.5]	-5.8 (-5.4) [-5.5]	This work
	ECP/t		-45.6			ref. ⁸
B3LYP	ECP/d	-68.3 (-64.5) [-66.4]	-46.7 (-45.1) [-45.2]	-13.3 (-12.6) [-12.7]	-5.9 (-5.5) [-5.6]	This work
	ECP/d	-62.0 (-58.1) [-60.0]	-40.9 (-38.2) [-39.4]	-10.3 (-9.6) [-10.0]		This work
	ECP/t		-41.90			ref. ⁸
CCSD(T) ^b	ECP/d	-63.0 (-59.1)	-41.9 (-39.2)			This work
CCSD(T)-F12b	see ref.	-66.64 (-62.67)	-46.9 (-45.2)	-14.9 (-14.1)		ref. ⁹⁻¹¹
expt. (0K, no ZPE)			-47.1			ref. ⁸
expt. (0K)		(-66.44)				ref. ¹²
expt. (298 K) ^c		[-66.91 ± 0.26]	[-45.2]	[-14.1]	[-6.1]	ref. ⁷

^aCalculated energies in kcal/mol. Values in normal text are electronic energy without zero-point energy (ZPE) correction; values in parentheses () are with ZPE correction; values in square brackets [] are with ZPE corrections and thermal corrections at 298.15 K.

^bThe values are single point energy calculated on top of structures optimized with B97-1/ECP/d method.

^cReaction enthalpy at 298.15 K.

References

1. R. A. Morris and A. A. Viggiano, *J. Phys. Chem.*, 1994, **98**, 3740-3746.
2. L. A. Angel and K. M. Ervin, *J. Phys. Chem. A*, 2001, **105**, 4042-4051.
3. E. Carrascosa, T. Michaelsen, M. Stei, B. Bastian, J. Meyer, J. Mikosch and R. Wester, *J. Phys. Chem. A*, 2016, **120**, 4711-4719.
4. D. M. Cyr, M. G. Scarton, K. B. Wiberg, M. A. Johnson, S. Nonose, J. Hirokawa, H. Tanaka, T. Kondow and R. A. Morris, *J. Am. Chem. Soc.*, 1995, **117**, 1828-1832.
5. L. A. Angel, S. P. Garcia and K. M. Ervin, *J. Am. Chem. Soc.*, 2002, **124**, 336-345.
6. L. A. Angel and K. M. Ervin, *J. Phys. Chem. A*, 2004, **108**, 9827-9833.
7. R. Otto, J. Xie, J. Brox, S. Trippel, M. Stei, T. Best, M. R. Siebert, W. L. Hase and R. Wester, *Faraday Discuss.*, 2012, **157**, 41-57.
8. J. Zhang and W. L. Hase, *J. Phys. Chem. A*, 2010, **114**, 9635-9643.
9. B. Olasz, I. Szabó and G. Czakó, *Chem. Sci.*, 2017, **8**, 3164-3170.
10. I. Szabo and G. Czako, *J. Phys. Chem. A*, 2017, **121**, 5748-5757.
11. D. A. Tasi, Z. Fábián and G. Czakó, *J. Phys. Chem. A*, 2018, **122**, 5773-5780.
12. R. C. Weast, *CRC Handbook of Chemistry and Physics*, 65th ed.; CRC Press: Boca Raton, FL, 2003.

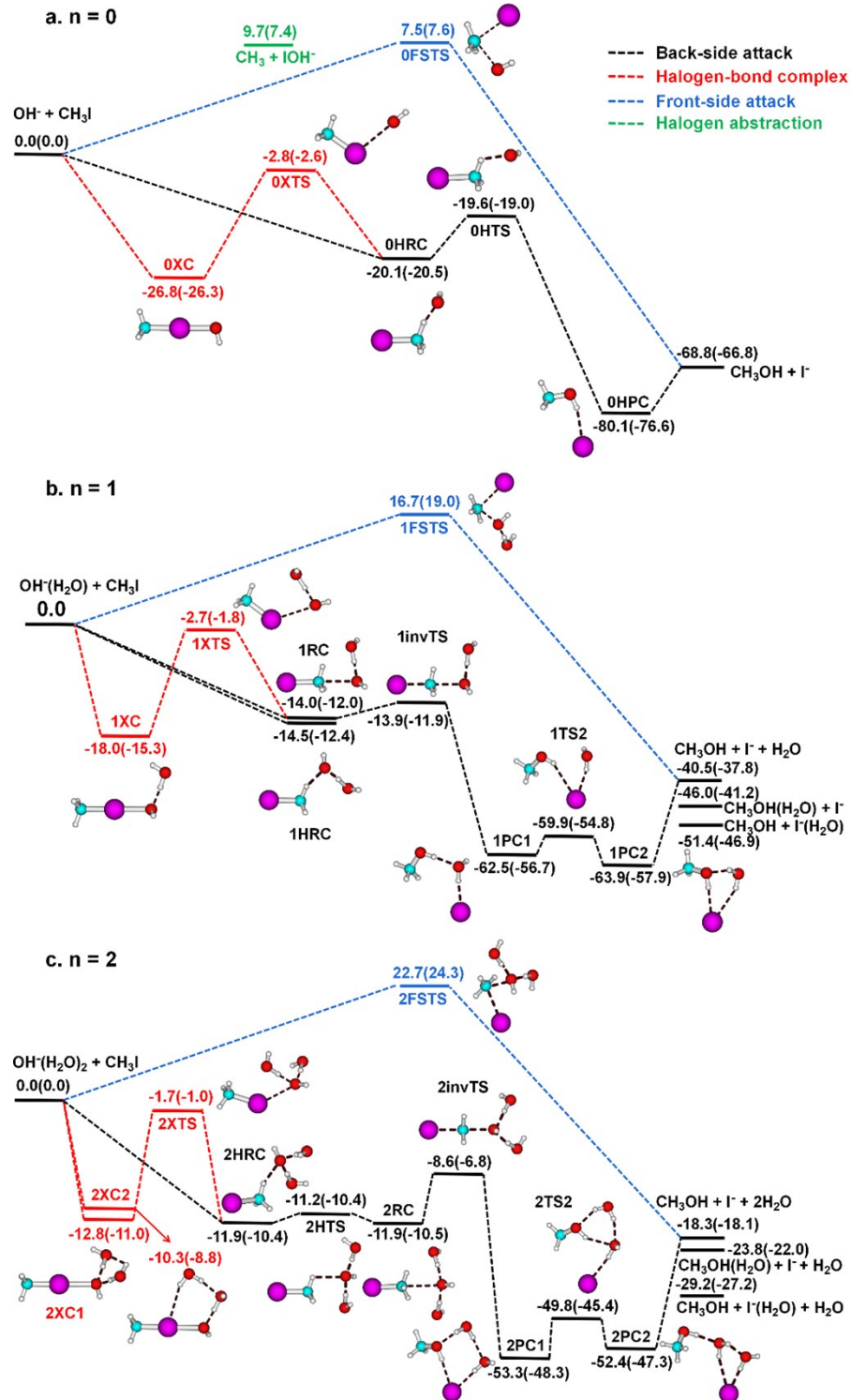


Figure S1. Potential energy profile of $\text{HO}^-(\text{H}_2\text{O})_{n=0,1,2} + \text{CH}_3\text{I}$ $\text{S}_{\text{N}}2$ reaction that displays the back-side attack, front-side attack, and halogen-bonded complex pathways using B97-1/ECP/d method. Energy values (in kcal/mol) without ZPE are in normal text and enthalpy values at 298.15 K are in parentheses. Color code: H, white; C, blue; O, red; I, pink.

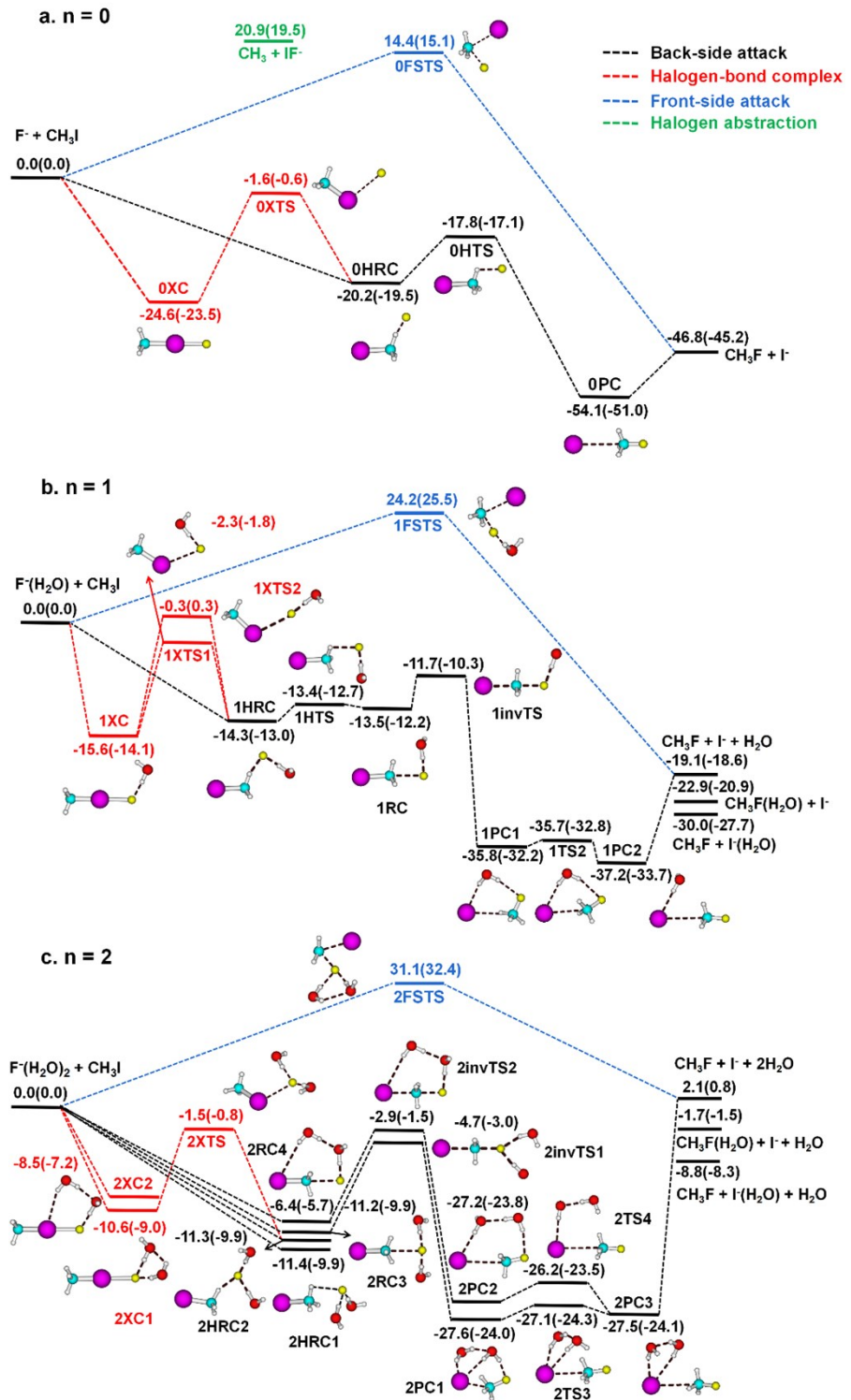


Figure S2. Potential energy profile of $F^-(H_2O)_{n=0,1,2} + CH_3I$ S_N2 reaction that displays the back-side attack, front-side attack, and halogen-bonded complex pathways using B97-1/ECP/d method. Energy values (in kcal/mol) without ZPE are in normal text and enthalpy values at 298.15 K are in parentheses. Color code: H, white; C, blue; O, red; F, yellow; I, pink.

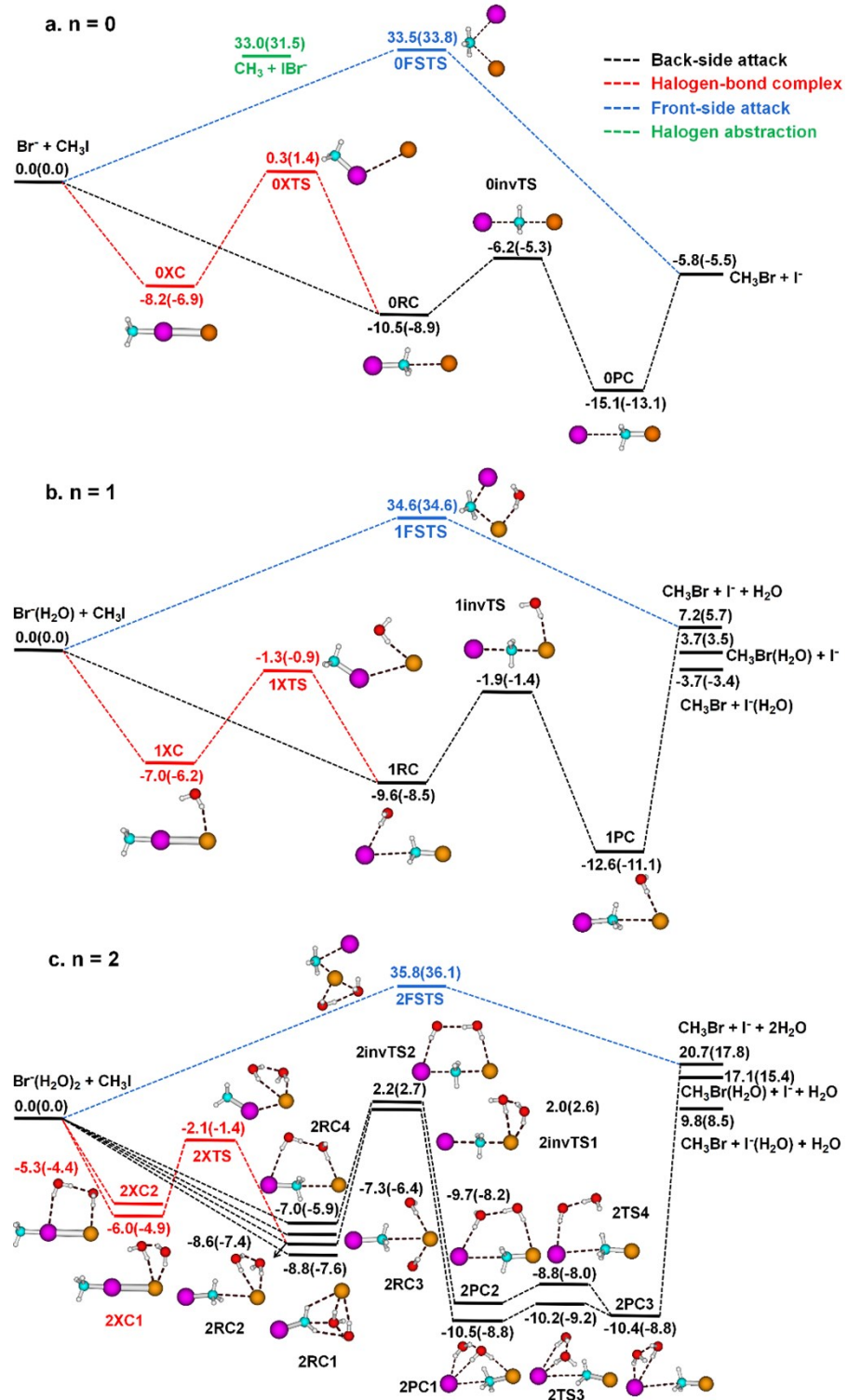


Figure S3. Potential energy profile of $\text{Br}^-(\text{H}_2\text{O})_{n=0,1,2} + \text{CH}_3\text{I}$ $\text{S}_{\text{N}}2$ reaction that displays the back-side attack, front-side attack, and halogen-bonded complex pathways using B97-1/ECP/d method. Energy values (in kcal/mol) without ZPE are in normal text and enthalpy values at 298.15 K are in parentheses. Color code: H, white; C, blue; O, red; Br, brown; I, pink.

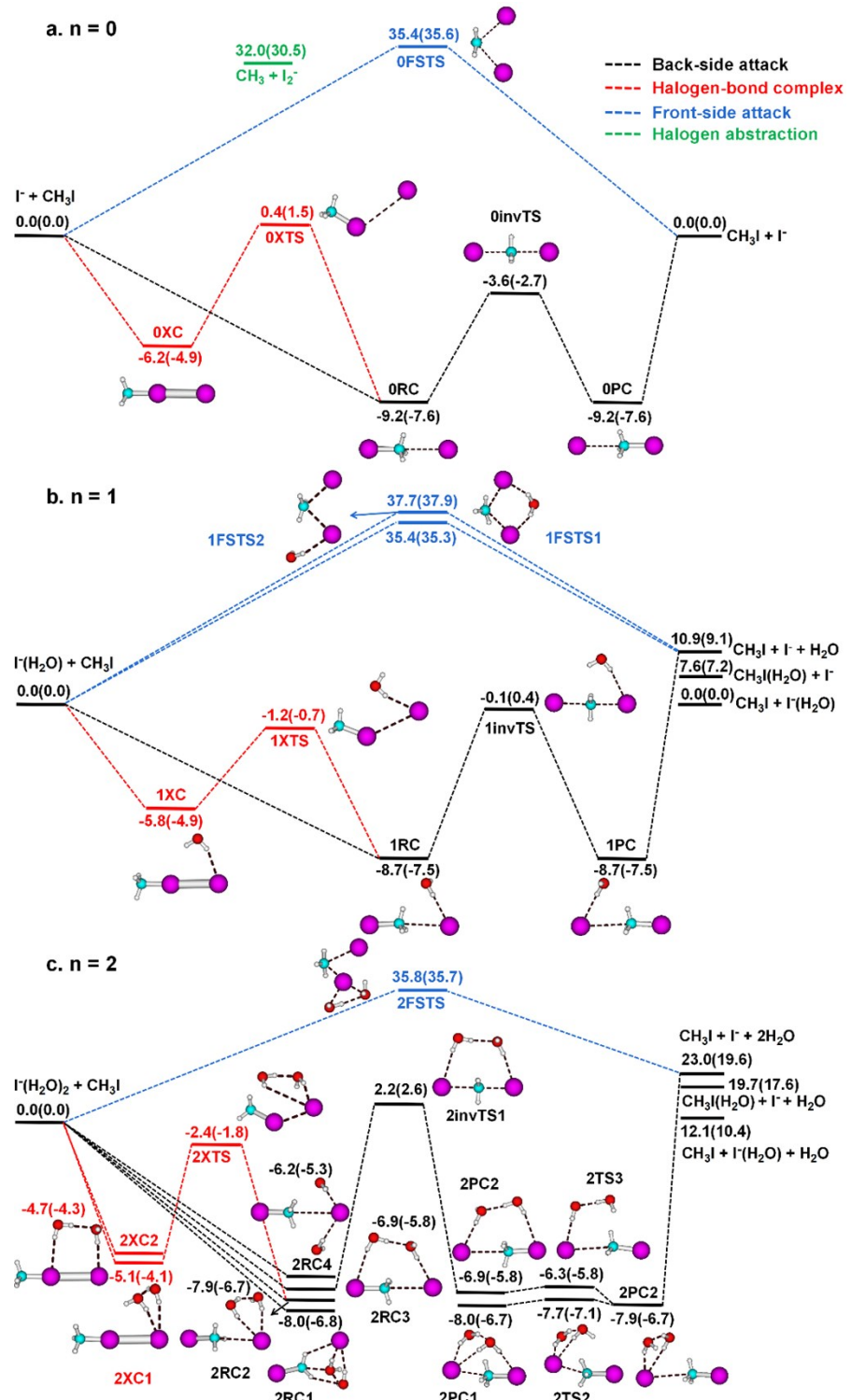
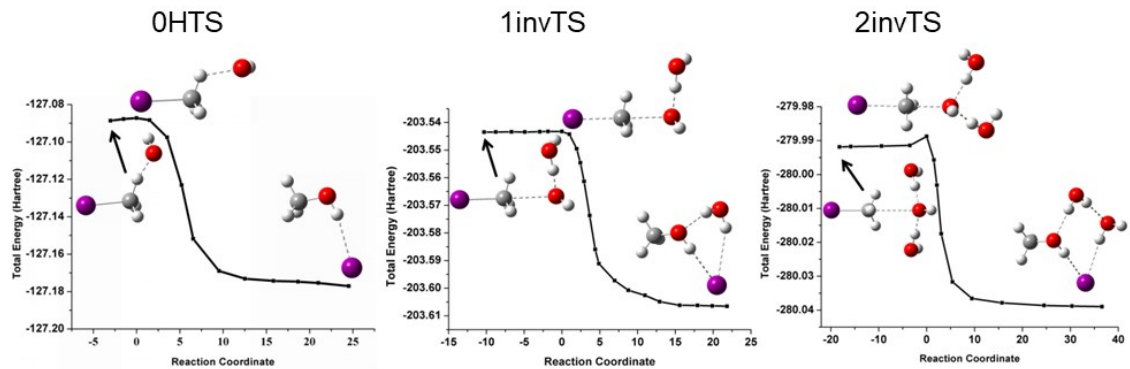
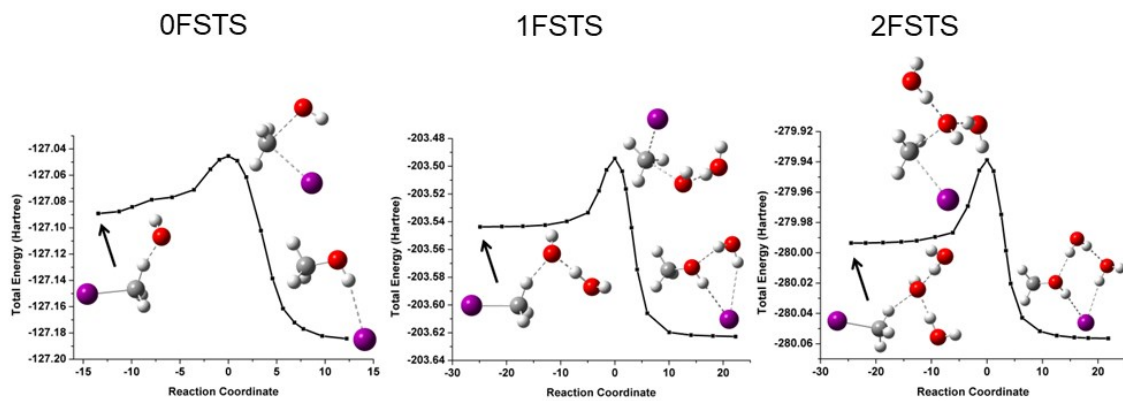


Figure S4. Potential energy profile of $\text{I}^-(\text{H}_2\text{O})_{n=0,1,2} + \text{CH}_3\text{I}$ $\text{S}_{\text{N}}2$ reaction that displays the back-side attack, front-side attack, and halogen-bonded complex pathways using B97-1/ECP/d method. Energy values (in kcal/mol) without zpe are in normal text and enthalpy values at 298.15 K are in parentheses. Color code: H, white; C, blue; O, red; I, pink.

a. back-side attack transition state



b. front-side attack transition state



c. halogen-bond complex transition state

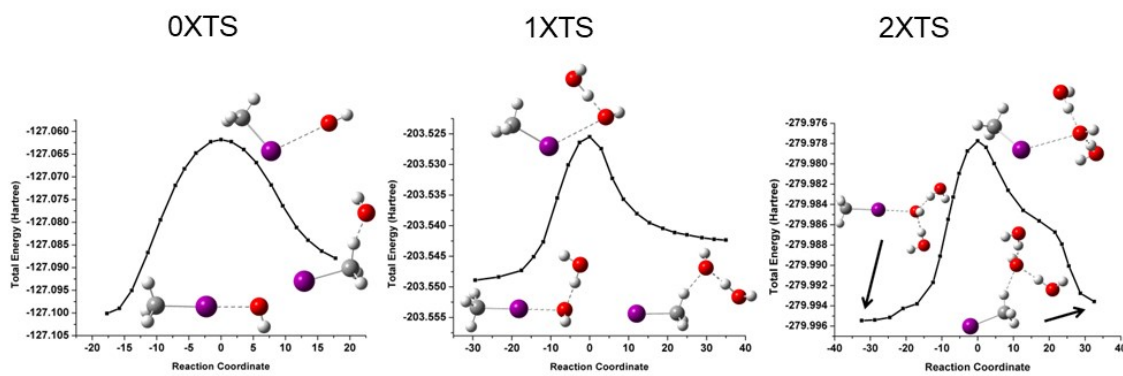
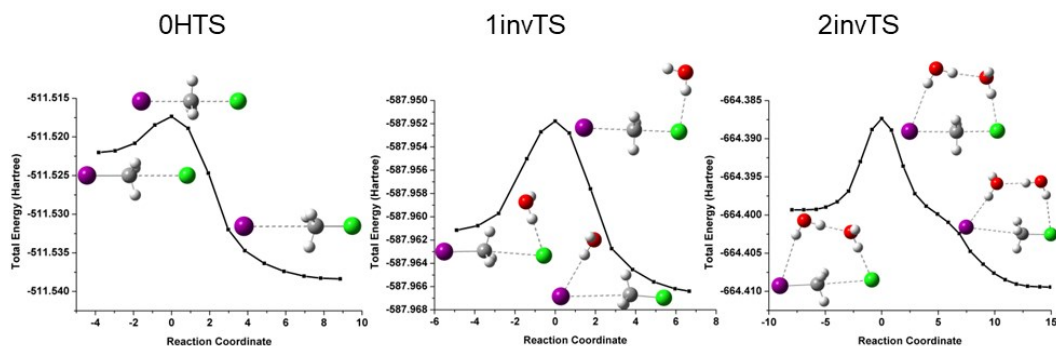
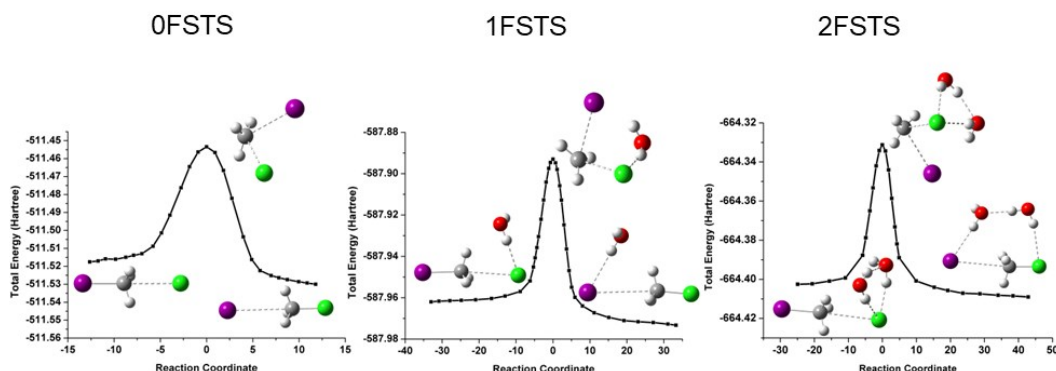


Figure S5. Intrinsic reaction coordinates (IRC) calculation of the invTS, FSTS, and XTS HO⁻(H₂O)_{n=0,1,2} + CH₃I S_N2 reaction using B97-1/ECP/d method.

a. back-side attack transition state



b. front-side attack transition state



c. halogen-bond complex transition state

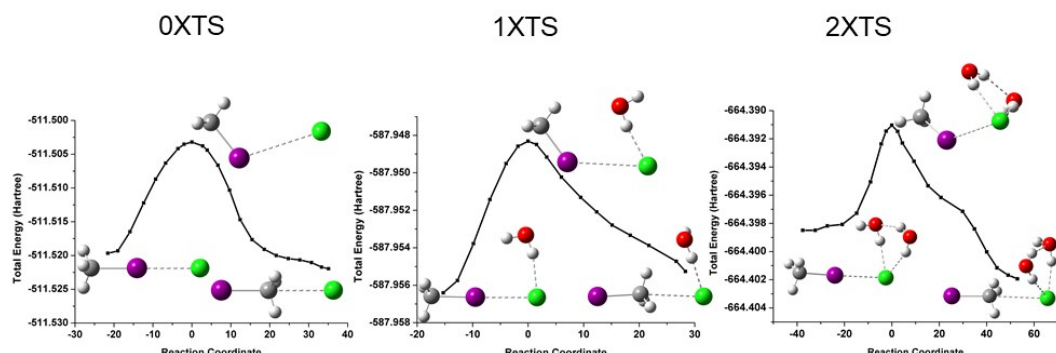


Figure S6. Intrinsic reaction coordinates (IRC) calculation of the invTS, FSTS, and XTS Cl⁻(H₂O)_{n=0,1,2} + CH₃I S_N2 reaction using B97-1/ECP/d method.

Table S3. Calculated energies (kcal/mol) of the stationary points relative to the reactants for the $\text{Y}^-(\text{H}_2\text{O})_{n=0,1,2} + \text{CH}_3\text{I}$ [$\text{Y} = \text{OH}, \text{F}, \text{Cl}, \text{Br}, \text{I}$] $\text{S}_{\text{N}}2$ reactions using B97-1/ECP/d. Values without zero-point-energy (ZPE) corrections are in normal text, values with ZPE corrections at 298.15 K are in parentheses.

	Nucleophile Y^-				
	HO^-	F^-	Cl^-	Br^-	I^-
$\text{Y}^- + \text{CH}_3\text{I}$	0.0	0.0	0.0	0.0	0.0
RC	-20.1 (-20.5)	-20.2 (-19.5)	-11.7 (-10.7)	-10.5 (-8.9)	-9.2 (-7.6)
invTS	-19.6 (-19.0)	-17.8 (-17.1)	-8.7 (-7.7)	-6.2 (-5.3)	-3.6 (-2.7)
PC	-80.1 (-76.6)	-54.1 (-51.0)	-21.9 (-19.6)	-15.1 (-13.1)	-9.2 (-7.6)
FSTS	7.5 (7.6)	14.4 (15.1)	31.4 (31.8)	33.5 (33.8)	35.4 (35.6)
XC	-26.8 (-26.3)	-24.6 (-23.5)	-10.2 (-8.9)	-8.2 (-6.9)	-6.2 (-4.9)
XTS	-2.8 (-2.6)	-1.6 (-0.6)	0.2 (1.2)	0.3 (1.4)	0.4 (1.5)
$\text{CH}_3\text{Y} + \text{I}^-$	-68.8 (-66.8)	-46.8 (-45.2)	-13.1 (-12.5)	-5.8 (-5.5)	0.0 (0.0)
$\text{XY}^- + \text{CH}_3$	9.7 (7.4)	20.9 (19.5)	32.7 (31.2)	33.0 (31.5)	32.0 (30.5)
	$\text{HO}^-(\text{H}_2\text{O})$	$\text{F}^-(\text{H}_2\text{O})$	$\text{Cl}^-(\text{H}_2\text{O})$	$\text{Br}^-(\text{H}_2\text{O})$	$\text{I}^-(\text{H}_2\text{O})$
$\text{Y}^-(\text{H}_2\text{O}) + \text{CH}_3\text{I}$	0.0	0.0	0.0	0.0	0.0
RC	-14.0 (-12.0)	-13.5 (-12.2)	-10.4 (-9.2)	-9.6 (-8.5)	-8.7 (-7.5)
invTS	-13.9 (-11.9)	-11.7 (-10.3)	-3.6 (-3.0)	-1.9 (-1.4)	-0.1 (0.4)
PC	-63.9 (-57.9)	-37.2 (-33.7)	-37.2 (-33.7)	-12.6 (-11.1)	-8.7 (-7.5)
FSTS	16.7 (19.0)	24.2 (25.5)	33.3 (33.4)	34.6 (34.6)	35.4 (35.3)
XC	-18.0 (-15.3)	-15.6 (-14.1)	-8.3 (-7.3)	-7.0 (-6.2)	-5.8 (-4.9)
XTS	-2.7 (-1.8)	-2.3 (-1.8)	-1.5 (-1.0)	-1.3 (-0.9)	-1.2 (-0.7)
$\text{CH}_3\text{Y} + \text{I}^- + \text{H}_2\text{O}$	-40.5 (-37.8)	-19.1 (-18.6)	1.9 (0.8)	7.2 (5.7)	10.9 (9.1)
	$\text{HO}^-(\text{H}_2\text{O})_2$	$\text{F}^-(\text{H}_2\text{O})_2$	$\text{Cl}^-(\text{H}_2\text{O})_2$	$\text{Br}^-(\text{H}_2\text{O})_2$	$\text{I}^-(\text{H}_2\text{O})_2$
$\text{Y}^-(\text{H}_2\text{O})_2 + \text{CH}_3\text{I}$	0.0	0.0	0.0	0.0	0.0
RC	-11.9 (-10.5)	-11.2 (-9.9)	-7.1 (-6.1)	-8.6 (-7.4)	-6.9 (-5.8)
invTS	-8.6 (-6.8)	-4.7 (-3.0)	0.4 (1.1)	2.0 (2.6)	2.2 (2.6)
PC	-52.4 (-47.3)	-27.5 (-24.1)	-14.2 (-12.3)	-10.4 (-8.8)	-7.9 (-6.7)
FSTS	22.7 (24.3)	31.1 (32.4)	35.6 (35.8)	35.8 (35.9)	35.8 (35.7)
XC	-12.8 (-11.0)	-10.6 (-9.0)	-6.6 (-5.6)	-6.0 (-4.9)	-5.1 (-4.1)
XTS	-1.7 (-1.0)	-1.5 (-0.8)	-1.9 (-1.3)	-2.1 (-1.4)	-2.4 (-1.8)
$\text{CH}_3\text{Y} + \text{I}^- + 2\text{H}_2\text{O}$	-18.3 (-18.1)	2.1 (0.8)	16.5 (13.8)	20.7 (17.8)	23.0 (19.6)

Table S4. Bond metrics for stationary points on back-side attack pathway of $\text{Y}^-(\text{H}_2\text{O})_{n=0,1,2} + \text{CH}_3\text{I}$ S_N2 reaction as calculated by B97-1/ECP/d level of theory. Bond distances are in Angstrom, angles are in degree, and imaginary frequency in cm⁻¹.

Y-	CH ₃ I	RC			invTS			imaginary frequency	PC			CH ₃ Y
		C-I	C-I	C-Y	∠I-C-Y	C-I	C-Y	∠I-C-Y	C-I	C-Y	∠I-C-Y	
n = 0												
HO ⁻	2.149	2.212	2.728	120.4	2.287	2.642	150.7	143i	3.994	1.413	62.4	1.425
F ⁻	2.149	2.200	2.674	118.3	2.257	2.532	155.8	145i	3.713	1.424	179.9	1.398
Cl ⁻	2.149	2.232	3.052	180.0	2.601	2.465	180.0	306i	3.613	1.848	180.0	1.809
Br ⁻	2.149	2.222	3.243	179.9	2.657	2.554	180.0	299i	3.553	2.007	179.8	1.959
I ⁻	2.149	2.211	3.513	179.8	2.714	2.712	180.0	291i	3.513	2.211	179.8	2.149
n = 1												
HO ⁻ (H ₂ O)	2.149	2.245	2.689	172.1	2.368	2.422	176.1	145i	4.001	1.419	59.9	1.419
F ⁻ (H ₂ O)	2.149	2.223	2.645	175.8	2.494	2.100	178.6	297i	3.844	1.421	174.2	1.398
Cl ⁻ (H ₂ O)	2.149	2.197	3.256	173.7	2.674	2.383	179.9	333i	3.781	1.839	173.0	1.809
Br ⁻ (H ₂ O)	2.149	2.193	3.431	173.1	2.712	2.492	178.8	309i	3.730	1.994	173.5	1.959
I ⁻ (H ₂ O)	2.149	2.189	3.706	173.9	2.738	3.673	176.2	290i	3.706	2.189	173.9	2.149
n = 2												
HO ⁻ (H ₂ O) ₂	2.149	2.191	2.954	175.6	2.482	2.232	178.8	330i	5.223	1.415	95.2	1.425
F ⁻ (H ₂ O) ₂	2.149	2.188	2.941	177.1	2.609	1.973	179.7	377i	3.895	1.419	171.4	1.398
Cl ⁻ (H ₂ O) ₂	2.149	2.196	3.196	176.8	2.697	2.354	178.5	333i	3.860	1.835	169.7	1.809
Br ⁻ (H ₂ O) ₂	2.149	2.183	3.535	169.7	2.772	2.431	178.4	300i	3.818	1.988	169.6	1.959
I ⁻ (H ₂ O) ₂	2.149	2.191	3.613	178.5	2.776	2.639	178.3	278i	3.613	2.191	178.5	2.149

Table S5. Bond metrics for front-side transition state on FSA pathway of $\text{Y}^-(\text{H}_2\text{O})_{n=0,1,2} + \text{CH}_3\text{I}$ $\text{S}_{\text{N}}2$ reaction as calculated by B97-1/ECP/d level of theory. Bond distances are in Angstrom, angles are in degree, and imaginary frequency in cm^{-1} .

Y^-	FSTS						
	C-I	C-Y	I-Y	$\angle \text{C}-\text{I}-\text{Y}$	$\angle \text{C}-\text{Y}-\text{I}$	$\angle \text{I}-\text{C}-\text{Y}$	imaginary frequency
$n = 0$							
HO^-	2.676	2.270	3.376	42.1	52.2	85.7	441i
F^-	2.704	2.018	3.081	40.2	59.8	80.0	476i
Cl^-	2.941	2.592	3.791	43.0	50.7	86.3	444i
Br^-	2.969	2.763	3.966	44.1	48.4	87.5	418i
I^-	2.996	2.996	4.190	45.6	45.6	88.7	401i
$n = 1$							
$\text{HO}^-(\text{H}_2\text{O})$	2.748	2.253	3.350	41.9	54.6	83.5	463i
$\text{F}^-(\text{H}_2\text{O})$	2.792	2.034	3.133	39.6	61.1	79.2	500i
$\text{Cl}^-(\text{H}_2\text{O})$	2.967	2.608	3.795	43.3	51.2	85.5	440i
$\text{Br}^-(\text{H}_2\text{O})$	2.979	2.768	3.950	44.4	48.9	86.7	415i
$\text{I}^-(\text{H}_2\text{O})$	3.002	3.002	4.167	46.1	46.1	87.8	396i
$n = 2$							
$\text{HO}^-(\text{H}_2\text{O})_2$	2.809	2.238	3.245	41.7	56.7	81.6	476i
$\text{F}^-(\text{H}_2\text{O})_2$	2.874	2.042	3.210	38.7	61.7	79.5	512i
$\text{Cl}^-(\text{H}_2\text{O})_2$	3.026	2.607	3.849	42.5	51.6	85.9	436i
$\text{Br}^-(\text{H}_2\text{O})_2$	3.047	2.774	4.010	43.7	49.4	86.9	407i
$\text{I}^-(\text{H}_2\text{O})_2$	3.061	3.008	4.214	45.5	46.5	88.0	393i

Table S6. Bond metrics for halogen-bonded complex and halogen-bonded transition state on XC pathway of $\text{Y}^-(\text{H}_2\text{O})_{n=0,1,2} + \text{CH}_3\text{I}$ $\text{S}_{\text{N}}2$ reaction as calculated by B97-1/ECP/d level of theory. Bond distances are in Angstrom, angles are in degree, and imaginary frequency in cm^{-1} .

Y ⁻	XC				XTS						imaginary frequency
	C-I	C-Y	I-Y	∠C-I-Y	C-I	C-Y	I-Y	∠C-I-Y	∠C-Y-I	∠I-C-Y	
n = 0											
HO ⁻	2.284	4.667	2.383	178.9	2.149	4.261	3.158	105.2	29.1	45.6	102i
F ⁻	2.240	4.556	2.316	180.0	2.144	4.290	3.186	105.5	28.8	45.7	101i
Cl ⁻	2.204	5.232	3.028	180.0	2.145	5.223	4.074	110.4	22.6	47.0	64i
Br ⁻	2.199	5.439	3.240	180.0	2.145	5.462	4.299	111.5	21.4	47.1	56i
I ⁻	2.196	5.719	3.523	180.0	2.146	5.806	4.617	113.1	19.9	47.0	51i
n = 1											
HO ⁻ (H ₂ O)	2.241	4.710	2.469	179.2	2.146	4.804	3.265	123.9	21.7	34.4	94i
F ⁻ (H ₂ O)	2.206	4.624	2.418	180.0	2.145	4.842	3.289	124.6	21.4	34.0	87i
Cl ⁻ (H ₂ O)	2.191	5.271	3.080	178.8	2.147	5.452	3.835	129.2	17.8	33.0	65i
Br ⁻ (H ₂ O)	2.189	5.475	3.286	178.7	2.149	5.638	3.993	130.9	16.8	32.4	61i
I ⁻ (H ₂ O)	2.188	5.745	3.557	178.3	2.150	5.912	4.228	133.2	15.4	31.4	54i
n = 2											
HO ⁻ (H ₂ O) ₂	2.210	4.765	2.555	179.1	2.146	4.902	3.348	124.9	21.0	34.1	80i
F ⁻ (H ₂ O) ₂	2.184	4.704	2.519	179.7	2.145	4.957	3.375	126.4	20.4	33.2	77i
Cl ⁻ (H ₂ O) ₂	2.180	5.319	3.139	178.5	2.148	5.479	3.809	131.7	17.0	31.3	65i
Br ⁻ (H ₂ O) ₂	2.180	5.511	3.332	178.1	2.150	5.651	3.939	134.2	15.8	30.0	54i
I ⁻ (H ₂ O) ₂	2.181	5.783	3.604	177.7	2.153	6.018	4.306	134.7	14.7	30.6	38i

Table S7. The ratio of the I-Y distance of the halogen-bonded complexes XC and transition state XTS to the sum of van der Waals radii of atom I and Y.

Y	n=0		n=1		n=2	
	XC	XTS	XC	XTS	XC	XTS
OH	0.66	0.88	0.68	0.91	0.71	0.93
F	0.66	0.90	0.68	0.93	0.71	0.96
Cl	0.75	1.02	0.77	0.96	0.78	0.95
Br	0.78	1.03	0.79	0.96	0.80	0.95
I	0.80	1.05	0.81	0.96	0.82	0.98

Table S8. Mulliken charge distribution for stationary points of $\text{Y}^-(\text{H}_2\text{O})_{n=0,1,2} + \text{CH}_3\text{I}$ $\text{S}_{\text{N}}2$ reaction as calculated by B97-1/ECP/d level of theory.

		invTS				FSTS				XC				XTS				
		Y	q(C)	q(I)	q(Y)	r(C-Y)	q(C)	q(I)	q(Y)	r(C-Y)	q(C)	q(I)	q(Y)	r(I-Y)	q(C)	q(I)	q(Y)	r(I-Y)
$n=0$	OH	0.582	-0.191	-0.797	2.642	0.677	-0.449	-0.676	2.270	0.439	0.047	-0.629	2.383	0.397	0.113	-0.924	3.158	
	F	0.543	-0.154	-0.865	2.532	0.756	-0.477	-0.636	2.018	0.478	0.070	-0.729	2.316	0.374	0.134	-0.937	3.186	
	Cl	0.506	-0.444	-0.675	2.465	0.680	-0.519	-0.617	2.592	0.476	0.078	-0.834	3.028	0.372	0.158	-0.980	4.074	
	Br	0.562	-0.480	-0.607	2.554	0.735	-0.525	-0.594	2.763	0.505	0.055	-0.850	3.240	0.370	0.160	-0.984	4.299	
	I	0.689	-0.498	-0.500	2.712	0.845	-0.535	-0.536	2.996	0.567	0.054	-0.867	3.523	0.357	0.172	-0.986	4.617	
$n=1$	OH	0.660	-0.292	-0.817	2.422	0.767	-0.470	-0.756	2.253	0.433	0.105	-0.678	2.469	0.406	0.161	-0.811	3.265	
	F	0.672	-0.343	-0.760	2.100	0.770	-0.502	-0.614	2.034	0.456	0.117	-0.734	2.418	0.385	0.170	-0.873	3.289	
	Cl	0.539	-0.500	-0.589	2.383	0.759	-0.514	-0.620	2.608	0.509	0.090	-0.814	3.080	0.385	0.189	-0.902	3.835	
	Br	0.686	-0.516	-0.543	2.492	0.776	-0.517	-0.594	2.768	0.524	0.085	-0.825	3.286	0.386	0.189	-0.901	3.993	
	I	0.874	-0.516	-0.436	2.673	0.877	-0.527	-0.527	3.002	0.557	0.091	-0.816	3.557	0.402	0.179	-0.889	4.228	
$n=2$	OH	0.689	-0.382	-0.926	2.232	0.867	-0.498	-0.991	2.238	0.327	0.261	-0.798	2.555	0.330	0.232	-0.891	3.348	
	F	0.781	-0.427	-0.701	1.973	0.852	-0.538	-0.603	2.042	0.486	0.135	-0.758	2.519	0.314	0.235	-0.825	3.375	
	Cl	0.674	-0.474	-0.593	2.354	0.880	-0.520	-0.622	2.607	0.541	0.086	-0.798	3.139	0.356	0.234	-0.860	3.809	
	Br	0.700	-0.549	-0.494	2.431	0.924	-0.514	-0.606	2.774	0.541	0.095	-0.809	3.332	0.363	0.230	-0.861	3.939	
	I	0.754	-0.487	-0.360	2.639	1.029	-0.507	-0.543	3.008	0.559	0.118	-0.801	3.604	0.456	0.189	-0.828	4.306	

Table S9. The charge transfer stabilization energy between lone pair of nucleophile Y⁻ and C-I antibonding σ^* orbital of the halogen-bonded complexes [CH₃--I--Y]⁻(H₂O)_{n=0,1,2} as calculated under NBO scheme.

Y	E _{stabilization} (kcal/mol)		
	n = 0	n = 1	n = 2
OH	36.25	26.32	16.66
F	29.71	18.88	10.25
Cl	14.51	12.35	9.98
Br	11.83	10.33	8.73
I	9.08	8.34	7.23

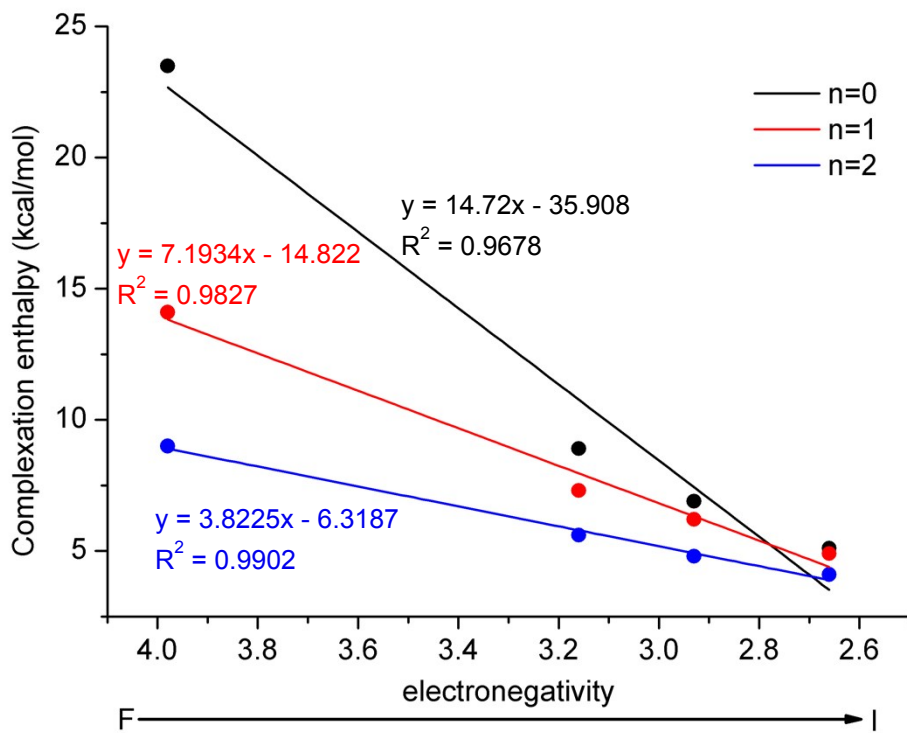


Fig. S7. Complexation enthalpies of halogen-bonded complexes as a function of electronegativity of halogen nucleophiles.

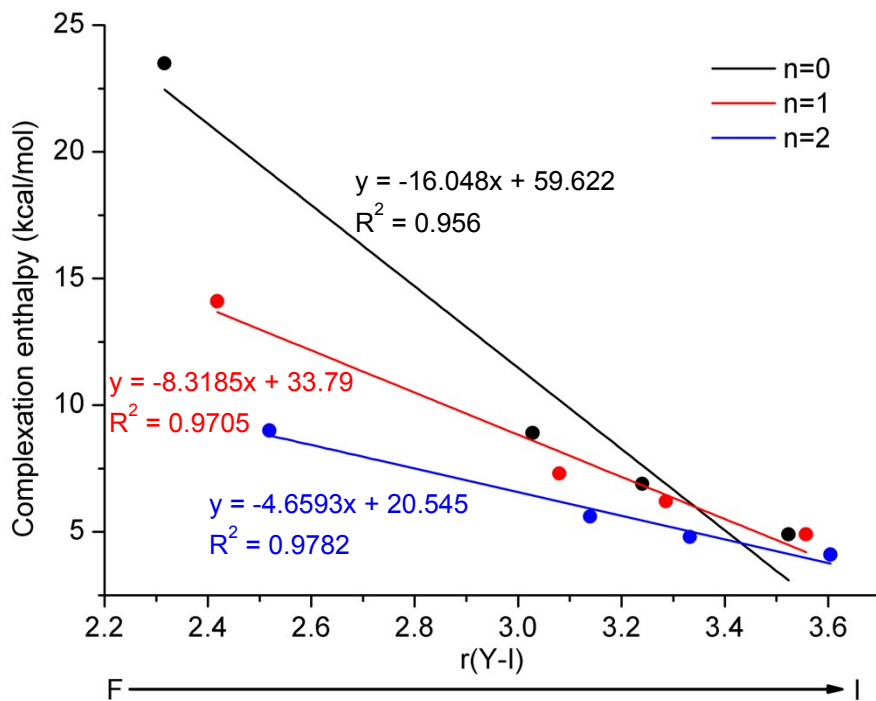


Fig. S8. Complexation enthalpies of halogen-bonded complexes as a function of Y-I distance of the halogen-bonded complexes $[\text{CH}_3\text{-I--Y}]^-(\text{H}_2\text{O})_{n=0,1,2}$.

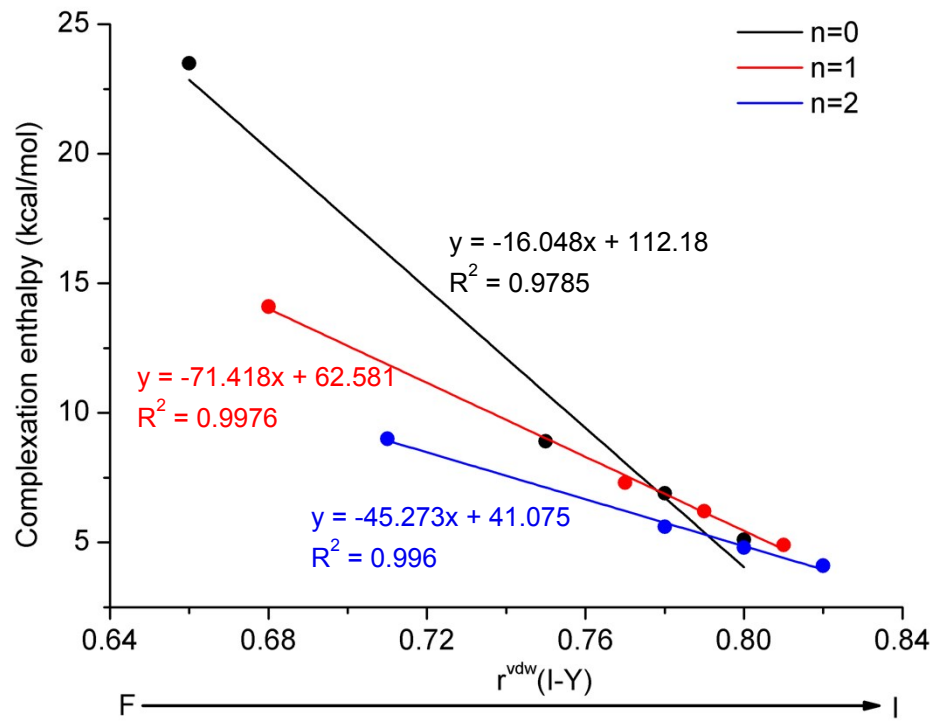


Fig. S9. Complexation enthalpies of halogen-bonded complexes as a function of $r^{vdw}(Y-I)$ of the halogen-bonded complexes $[CH_3--I--Y] \cdot (H_2O)_{n=0,1,2}$.

Table S10. Calculated energies (kcal/mol) of the stationary points relative to the reactants for the $\text{Y}^-(\text{H}_2\text{O})_{n=0,1,2} + \text{CH}_3\text{I}$ [$\text{Y} = \text{OH}, \text{F}, \text{Cl}, \text{Br}, \text{I}$] $\text{S}_{\text{N}}2$ reactions. Structures are optimized using B97-1/ECP/d method and implicit solvent model PCM with water as solvent. Values without zero-point-energy (ZPE) corrections are in normal text, values with ZPE corrections at 298.15 K are in parentheses.

	Nucleophile Y^-				
	HO^-	F^-	Cl^-	Br^-	I^-
$\text{Y}^- + \text{CH}_3\text{I}$	0.0	0.0	0.0	0.0	0.0
RC	-2.3 (-1.3)	-2.1 (-0.4)	-0.5 (1.3)	-0.5 (1.2)	-0.6 (1.2)
invTS	-	7.8 (9.0)	13.3 (14.4)	13.4 (14.3)	13.1 (13.9)
PC	-53.0 (-49.5)	-23.7 (-20.5)	-4.3 (-1.9)	-1.3 (0.2)	-0.6 (1.2)
FSTS	32.5 (32.6)	35.5 (40.3)	46.6 (47.0)	46.4 (46.7)	45.9 (46.2)
XC	-3.2 (-4.7)	-3.2 (-1.6)	-1.5 (0.2)	-1.6 (0.1)	-1.5 (0.2)
<u>a</u> XTS	<u>5.0 (5.2)</u>	<u>5.3 (6.3)</u>	<u>1.2 (2.3)</u>	<u>0.7 (1.9)</u>	<u>0.3 (1.4)</u>
$\text{CH}_3\text{Y} + \text{I}^-$	-47.5 (-49.3)	-23.0 (-21.5)	-3.6 (-3.0)	-0.7 (-0.4)	0.0 (0.0)
	$\text{HO}^-(\text{H}_2\text{O})$	$\text{F}^-(\text{H}_2\text{O})$	$\text{Cl}^-(\text{H}_2\text{O})$	$\text{Br}^-(\text{H}_2\text{O})$	$\text{I}^-(\text{H}_2\text{O})$
$\text{Y}^-(\text{H}_2\text{O}) + \text{CH}_3\text{I}$	0.0	0.0	0.0	0.0	0.0
RC	-2.0 (-0.5)	-1.3 (-0.1)	-1.2 (0.1)	-1.1 (0.1)	-1.1 (0.1)
invTS	5.6 (7.2)	10.3 (11.4)	14.5 (15.1)	14.4 (14.9)	13.8 (14.1)
PC	-44.4 (-39.5)	-17.3 (-13.1)	-3.1 (-1.3)	-0.9 (0.6)	-1.1 (0.1)
FSTS	35.1 (36.3)	42.0 (42.7)	46.5 (46.4)	46.0 (45.8)	45.1 (44.8)
XC	-3.6 (-2.0)	-2.5 (-1.2)	-1.8 (-0.6)	-1.9 (-0.7)	-2.0 (-0.8)
<u>a</u> XTS	<u>4.0 (4.9)</u>	<u>2.8 (3.3)</u>	<u>1.2 (1.7)</u>	<u>0.8 (1.2)</u>	<u>0.2 (0.7)</u>
$\text{CH}_3\text{Y} + \text{I}^- + \text{H}_2\text{O}$	-36.0 (-34.1)	-11.6 (-11.5)	1.5 (0.4)	3.7 (2.3)	3.5 (1.8)
	$\text{HO}^-(\text{H}_2\text{O})_2$	$\text{F}^-(\text{H}_2\text{O})_2$	$\text{Cl}^-(\text{H}_2\text{O})_2$	$\text{Br}^-(\text{H}_2\text{O})_2$	$\text{I}^-(\text{H}_2\text{O})_2$
$\text{Y}^-(\text{H}_2\text{O})_2 + \text{CH}_3\text{I}$	0.0	0.0	0.0	0.0	0.0
RC	-1.9 (-0.6)	-1.8 (-0.4)	-2.8 (-0.9)	-2.2 (-1.0)	-2.2 (-1.0)
invTS	7.1 (8.5)	12.8 (14.0)	13.2 (14.0)	13.7 (13.2)	13.3 (13.7)
PC	-38.3 (-33.5)	-11.6 (-8.5)	-4.4 (-1.8)	-1.8 (-0.2)	-2.2 (-1.0)
FSTS	37.1 (38.2)	43.7 (44.3)	46.6 (47.0)	45.5 (45.4)	44.3 (44.1)
XC	-3.1 (-1.7)	-2.2 (-1.0)	-2.9 (-1.1)	-2.4 (-1.3)	-2.6 (-1.5)
<u>a</u> XTS	<u>2.9 (3.6)</u>	<u>2.3 (3.0)</u>	<u>1.0 (1.7)</u>	<u>0.7 (1.4)</u>	<u>-0.5 (0.1)</u>
$\text{CH}_3\text{Y} + \text{I}^- + 2\text{H}_2\text{O}$	-34.6 (-24.5)	-2.1 (-3.5)	6.3 (4.4)	6.0 (8.9)	8.3 (5.1)

^aThe structure of XTS cannot be optimized using PCM implicit solvent model, so we performed single point calculation on top of gas-phase optimized structure.

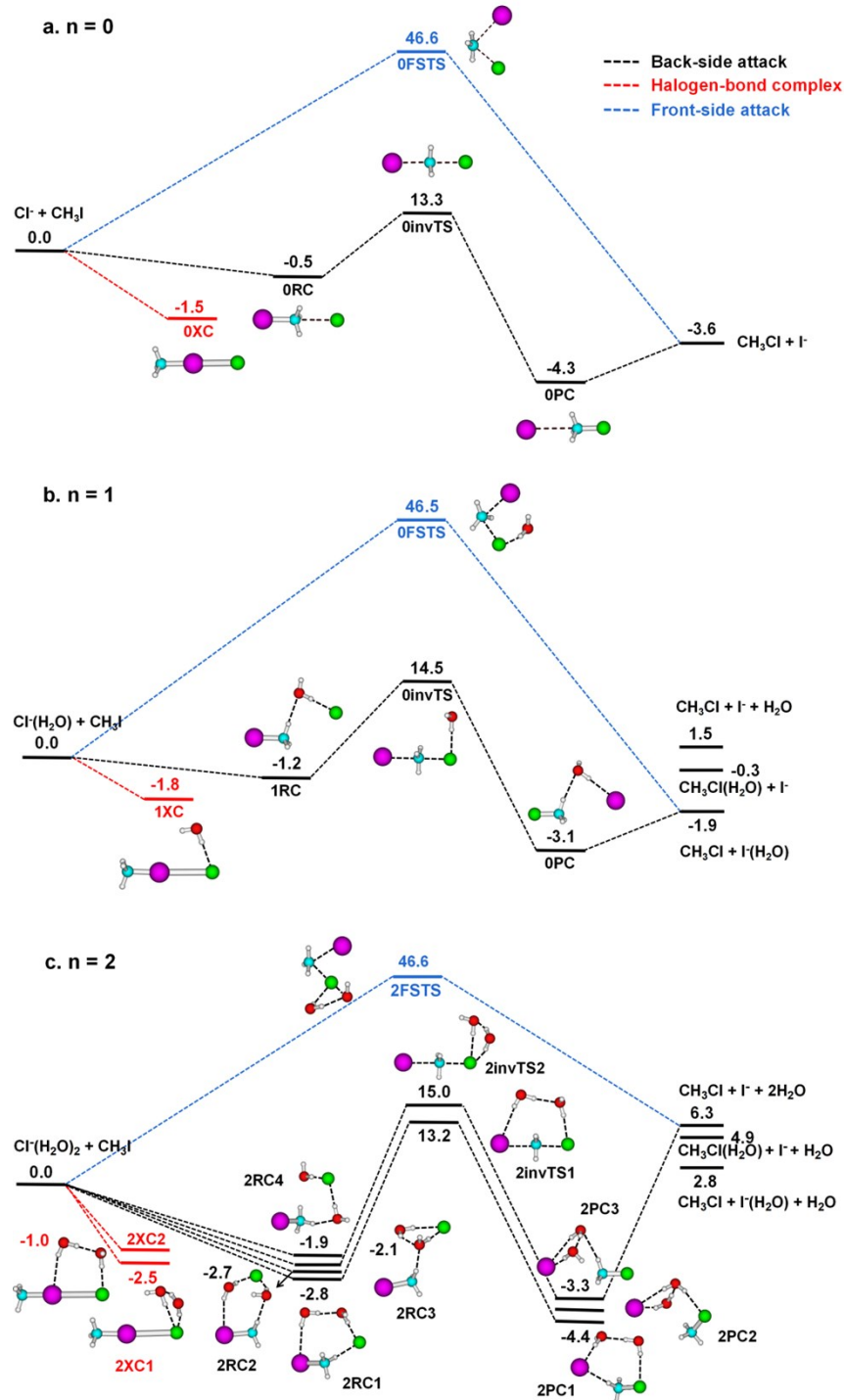


Figure S10. Potential energy profile of $\text{Cl}^-(\text{H}_2\text{O})_{n=0,1,2} + \text{CH}_3\text{I}$ $\text{S}_{\text{N}}2$ reaction that displays the back-side attack, front-side attack, and halogen-bonded complex pathways using B97-1/ECP/d method. Structures are optimized using implicit solvent model PCM with water as solvent. Energies (in kcal/mol) are electronic energy without zero-point energy. Color code: H, white; C, blue; O, red; Cl, green; I, pink.

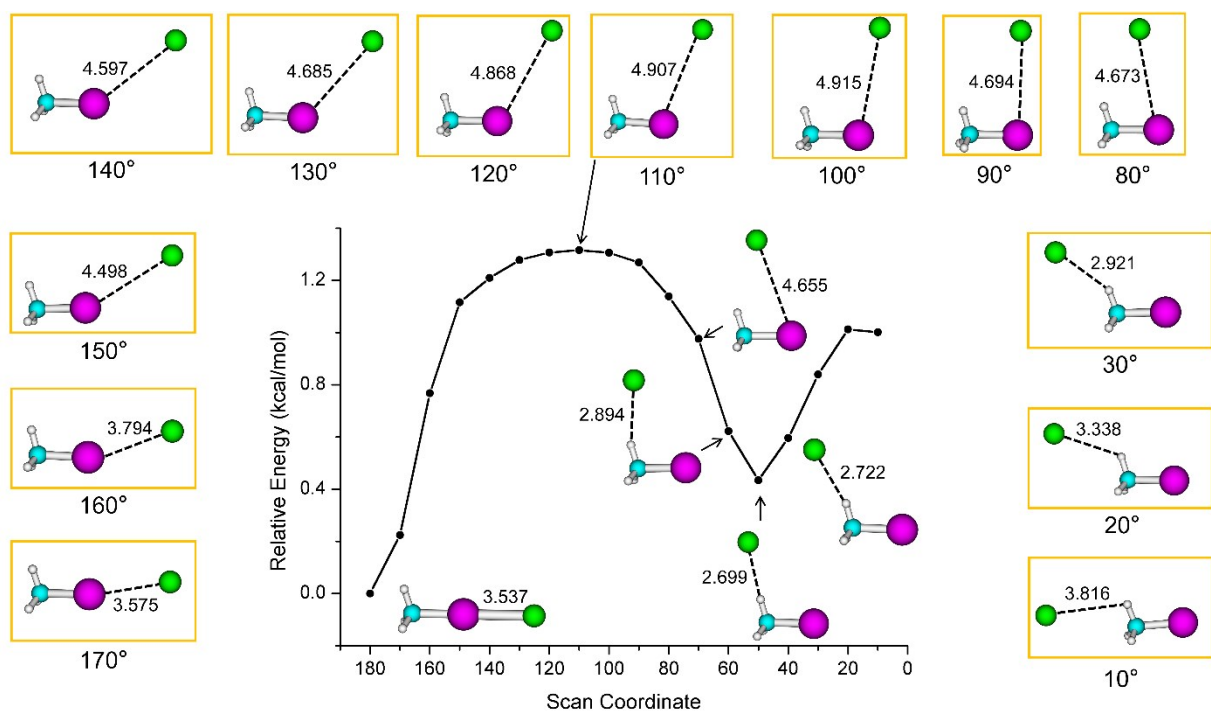


Fig. S11. Energy profile of scanning C-I-Cl bond angle of halogen-bonded complex $[\text{CH}_3\text{--I--Cl}]^-$. The angles are in degree and distances are in angstrom. Color code: H, white; C, green; Cl, green; I, pink.

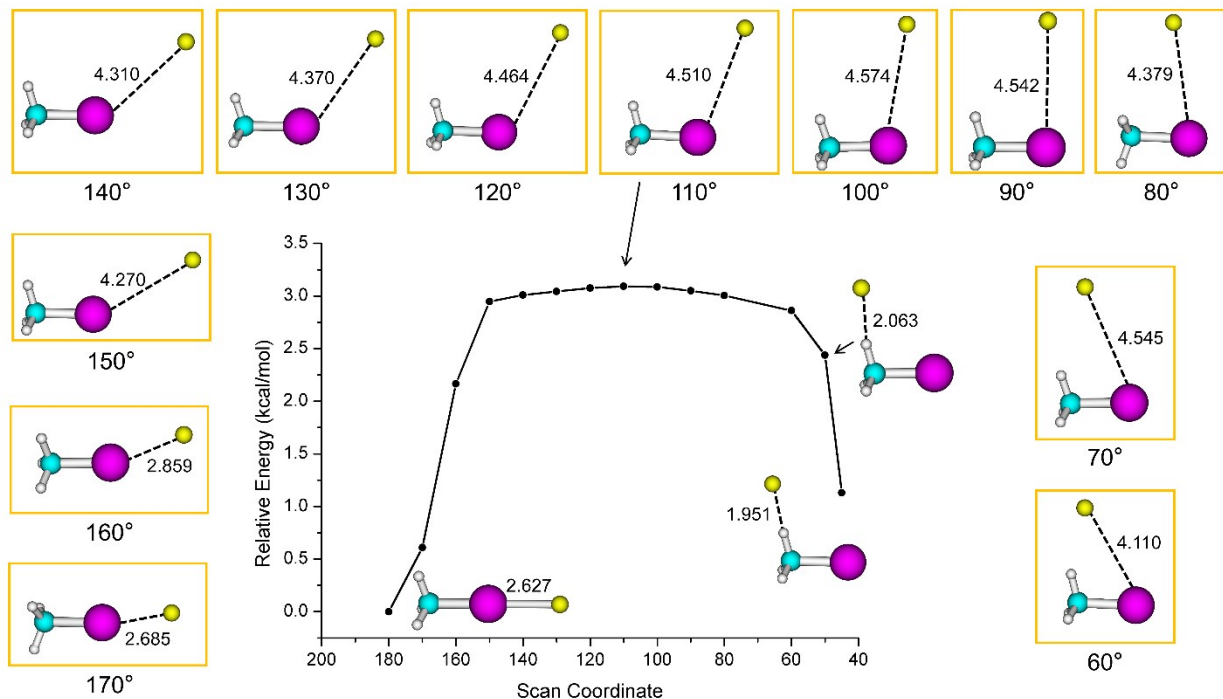


Fig. S12. Energy of profile of scanning C-I-F bond angle of halogen-bonded complex $[\text{CH}_3\text{--I--F}]^-$. The angles are in degree and distances are in angstrom. Color code: H, white; C, green; F, yellow; I, pink.